Thermodynamics and Kinetics of Methylboroxine·Amine Adduct Formation: A Computational Study

Jeremy Kua* and Charles R. Gyselbrecht

Department of Chemistry, University of San Diego, 5998 Alcala Park, San Diego, California 92110

Received: January 31, 2007; In Final Form: March 23, 2007

Density functional theory (B3LYP//6-311+G*) calculations including Poisson−Boltzmann implicit solvent were applied to study the formation of the trimethylboroxine·amine adduct with respect to methylboronic acid monomers and free amine in solution. Potential intermediates and transition states between intermediates were calculated to assess the thermodynamic and kinetic factors controlling this transformation. Our calculations suggest that the rate-determining steps are condensation reactions to form dimers and trimers, and closure of the boroxine ring. Fast amine exchange is expected throughout the transformation, and the most-stable intermediate is a dimer·amine adduct. Using our calculated barriers for the methyl system as a template, we assess the conversion of phenylboronic acid to the triphenylboroxine·amine adduct and find that the pathway is most likely similar, except that the transformation is thermodynamically and kinetically more favored for the phenyl system in the presence of pyridine.

Introduction

Boroxines, the dehydration product of organoboronic acids,[1] have found commercial use in such diverse areas as flame-retardant materials,[2] dopants for lithium ion transference in polymer electrolytes,[3−5] acid alternatives in Suzuki−Miyaura coupling reactions,[6] and nonlinear optical materials.[7] Boroxines are known to form stable adducts with many nitrogen-donor compounds including amines,[8−12] pyridines,[13] hydrazines,[14] azaindoles,[15] and even salen-type ligands.[16] Arylboroxines are also finding increased utility in material-science applications, such as covalent organic frameworks,[17] borane-end functionalized polymers,[18] and nanoscale molecular scaffolds.[19]

There are few studies investigating the thermodynamics of forming boroxine from boronic acids. Figure 1 shows a two-step reaction sequence separating the effect of a nitrogen-donor compound. Boroxine is constructed from monomeric boronic acid in step 1, and boroxine subsequently forms an adduct with nitrogen-donor compounds in step 2. The equilibrium constant between phenylboronic acid and triphenylboroxine for a series of *para*-phenyl substituents in the absence of ligands (corresponding to step 1) has been measured by NMR.[20]

In a previous computational study, we examined the effect of the para substituent on the thermodynamics of each step.[21] We found that the trimerization of phenylboronic acids to form arylboroxine rings (step 1) is enthalpically unfavorable. In contrast, the formation of stable 1:1 adducts (step 2) was highly favorable and, in fact, sufficiently favorable to drive the two-step reaction forward toward formation of the products. Substitution of π-electron-withdrawing groups in the para position of the phenyl ring further disfavored step 1, whereas the opposite was observed for π-electron donors. Alternatively, substituents that were *overall* electron-withdrawing favored step 2, whereas electron donors disfavored it. We also found that the formation of 1:2 adducts of arylboroxine·amine were less favorable enthalpically compared to 1:1 adducts. In a computational study prior to ours, the relief of ring strain was proposed to explain the stability of boroxine·amine adducts,[22] although our study did not find evidence in favor of the ring strain argument.

We then examined the enthalpy changes of intermediate steps to identify potential stable intermediates using both computational methods and NMR.[23] From our calculations we found that, in the absence of amine, the formation of Lewis-acid oligomers (dimer, linear trimer, boroxine ring) is enthalpically unfavorable. Although the formation of a monomer·amine adduct was marginally endothermic, formation of adducts with the dimer and boroxine ring was exothermic. Stronger electron-withdrawing para substituents led to further stabilization of the adduct. NMR data provided independent confirmation that electron-withdrawing substituents drive the two-step equilibrium toward adduct formation, in agreement with our computational results.

Our calculations suggested that the most important intermediate en route to forming the boroxine·amine adduct is the dimer·amine adduct. Formation of the dimer·amine adduct can proceed via two pathways. Electron-donating substituents favored dimerization of two monomers before the addition of amine, whereas electron-withdrawing substituents favored formation of the monomer·amine adduct prior to the addition of the second monomer.

The conclusions drawn from our previous studies only considered the relative enthalpic stability of reactants, products, and intermediates but did not address the energy barriers required for transformation between chemical species. The present work begins to address this issue. We have calculated the relevant energy barriers and transition-state structures for the transformation of methylboronic acid into the trimethylboroxine·NH_3 adduct.

The main reactions studied are shown in Figure 2, which also depicts the reactants, products, and stable intermediates considered in this study. The Lewis-acid monomer, dimer, and linear trimer are labeled **1**, **2**, and **3** respectively. The boroxine ring is distinguished from the open trimer by the label **3r**. The adducts

* Corresponding author. E-mail: jkua@sandiego.edu.

10.1021/jp0708594 CCC: $37.00
Published on Web 05/16/2007

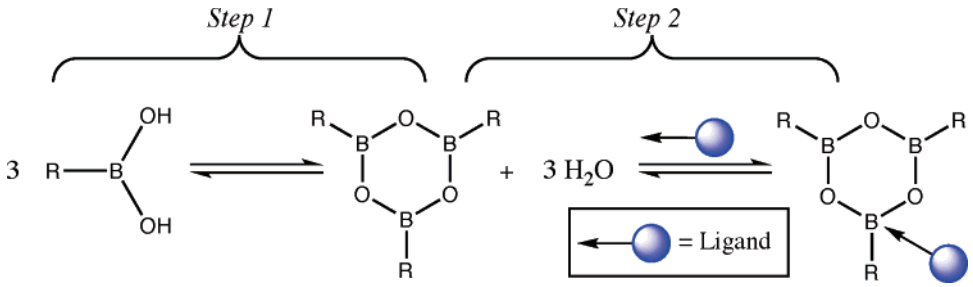

Figure 1. Two-step reaction sequence of boroxine construction followed by adduct formation.

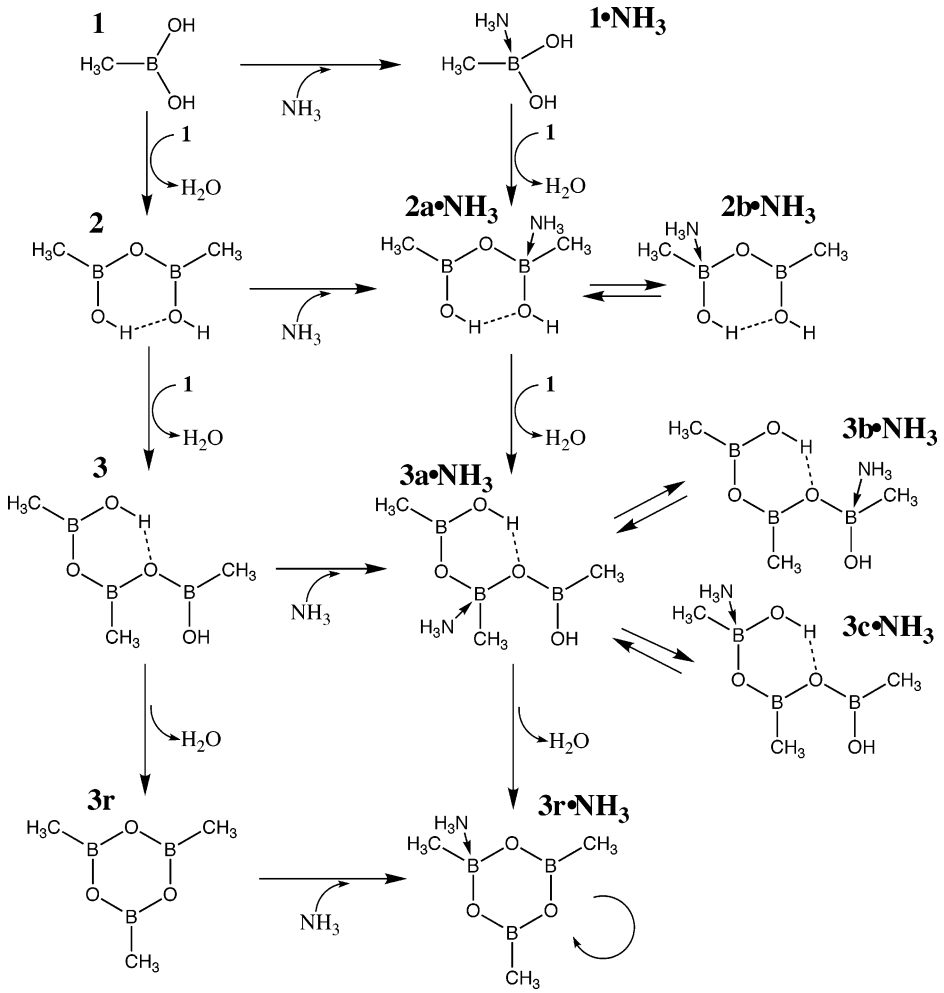

Figure 2. Potential reactions and intermediates in the conversion of methylboronic acid to the trimethylboroxine·NH_3 adduct.

are labeled with the appropriate ·**NH_3** suffix. In the case of the dimer and open trimer adducts, NH_3 can ligate to nonequivalent boron centers. The nonequivalency arises from the hydrogen bond between the two hydroxyl groups in the dimer and between one of the hydroxyl groups and one of the B−O−B oxygens in the trimer. The lowest-energy intermediate is designated **a**, the next lowest, **b**, and so on.

There are few studies investigating the kinetics of this system. To our knowledge, the only low-temperature NMR studies examined the fast exchange of ligands in boroxine·amine adducts. The experimentally determined activation barriers are 9−13 kcal/mol.[15,24,25] Our calculated hopping barriers of the amine ligand on the boroxine ring are in this range.

To locate transition states rapidly, we chose to calculate the barriers for conversion of methylboronic acid to trimethylboroxine·NH_3 rather than from phenylboronic acid to triphenylboroxine·pyridine. However, in this study, we make direct comparisons between the present calculations with methyl and our previous calculations with phenyl,[23] at least for all of the intermediates shown in Figure 2. To compare barriers between the methyl and phenyl systems (and take into account the difference between NH_3 and pyridine), we chose to calculate just three transition states of the phenyl system and the pyridine ligand: the ligand ring-hopping reaction of **3r·pyr**, the conversion of **1** to **1·pyr**, and the dimerization reaction converting **1** to **2**. A comparison between NH_3 and pyridine with respect to the thermodynamics for the formation of 1:1 adducts with triphenylboroxine can also be found in our previous study.[21]

Materials and Methods

Computational Methods. All calculations were carried out using Jaguar 5.5[26] at the B3LYP[27−30] density functional theory with a 6-311+G* basis set. We chose to run our calculations at a similar level of theory and basis set to complement our

TABLE 1: Thermodynamics of Methylboroxine·NH_3 Formation from Methylboronic Acid

reaction		ΔE_{elec} (kcal/mol)	ΔE_{solv} (kcal/mol)	ΔE_{corr} (kcal/mol)	ΔH_{soln} (kcal/mol)
1 + **1** → **2** + H_2O	dimerization	4.25	1.28	−0.53	5.00
2 + **1** → **3** + H_2O	trimerization	8.62	−0.58	−0.72	7.32
3 → **3r** + H_2O	ring closure	5.13	−4.59	−3.86	−3.32
1 + NH_3 → **1·NH$_3$**	addition of NH_3	1.00	−2.26	1.56	0.30
2 + NH_3 → **2a·NH$_3$**	addition of NH_3	−4.27	−3.48	1.61	−6.14
3 + NH_3 → **3a·NH$_3$**	addition of NH_3	−6.93	−4.25	2.43	−8.75
3r + NH_3 → **3r·NH$_3$**		−7.04	−6.42	4.15	−9.31
2a·NH$_3$ → **2b·NH$_3$**	NH_3 hop	2.27	−0.39	0.34	2.22
3a·NH$_3$ → **3b·NH$_3$**	NH_3 hop	2.06	−0.44	−0.30	1.32
3a·NH$_3$ → **3c·NH$_3$**	NH_3 hop	4.87	−0.31	−1.11	3.45

TABLE 2: Thermodynamics of Phenylboroxine·NH_3 Formation from Phenylboronic Acid

reaction		ΔE_{elec} (kcal/mol)	ΔE_{solv} (kcal/mol)	ΔE_{corr} (kcal/mol)	ΔH_{soln} (kcal/mol)
1 + **1** → **2** + H_2O	dimerization	2.76	1.31	−0.90	3.17
2 + **1** → **3** + H_2O	trimerization	7.08	−0.28	0.00	6.80
3 → **3r** + H_2O	ring closure	3.37	−4.71	−1.84	−3.18
1 + NH_3 → **1·NH$_3$**	addition of NH_3	−0.32	−1.44	1.83	0.07
2 + NH_3 → **2a·NH$_3$**	addition of NH_3	−2.59	−3.52	2.23	−3.88
3 + NH_3 → **3a·NH$_3$**	addition of NH_3	−8.52	−3.30	2.42	−9.40
3r + NH_3 → **3r·NH$_3$**		−6.45	−4.34	2.20	−8.59
2a·NH$_3$ → **2b·NH$_3$**	NH_3 hop	0.48	1.32	0.26	2.06
3a·NH$_3$ → **3b·NH$_3$**	NH_3 hop	5.62	0.10	−0.90	4.82
3a·NH$_3$ → **3c·NH$_3$**	NH_3 hop	6.31	0.76	−1.17	5.90

previous studies.[21,23] The electronic energy of the optimized gas-phase structures is designated E_{elec}. The Poisson−Boltzmann (PB) continuum approximation[31,32] was used to describe the effect of the solvent. In this approximation, a smooth solvent-accessible surface of the solute is calculated by rolling a sphere of radius R_{solv} over the van der Waals surface. The solvent is represented as a polarizable continuum surrounding the molecule with dielectric constant ϵ. Charges are allowed to develop on the surface according to the electrostatic potential of the solute and ϵ; then the polarized reaction field of the solvent acts back on the quantum-mechanical description of the solute. The wave function of the complex is relaxed self-consistently with the reaction field to solve the PB equations. Although the forces on the quantum-mechanical solute atoms due to the solvent can be calculated in the presence of the solvent, in this work the solvation energy was calculated at the optimized gas-phase geometry for all structures at minima. This is because there is little change between the gas-phase and implicit solvent-optimized geometries. For transition states, we used two different strategies (described later). The difference in energy between the unsolvated and solvated structures is designated E_{solv}.

The parameters used for the dielectric constant and probe radius are $\epsilon = 80.4$ and $R_{solv} = 1.40$ Å for water, $\epsilon = 10.0$ and $R_{solv} = 2.33$ Å for dichloromethane. We chose to use water as the implicit solvent for all calculations using the methyl group and NH_3 as in our first study.[21] For calculations using phenyl and pyridine, we used dichloromethane as the solvent for comparison with experimental NMR results. A further comparison of the effect of different solvents on the thermodynamics can be found in our previous computational and NMR study.[23]

The analytical Hessian was calculated for each optimized geometry in the gas phase. The DFT gas-phase energy was then corrected for zero-point vibrations. Negative eigenvalues in transition-state calculations were not included in the zero-point energy. The temperature-dependent enthalpy correction term is straightforward to calculate from statistical mechanics. Assuming that the translational and rotational corrections are a constant times kT, that low-frequency vibrational modes will generally cancel out when calculating enthalpy differences, and that the vibrational frequencies do not change appreciably in solution, we can calculate H_{298K}. The sum of the zero-point energy and enthalpy corrections to 298 K are collectively designated E_{corr}. The calculated values of E_{elec}, E_{solv}, and E_{corr} are available in the Supporting Information. The corresponding free-energy corrections in solution are much-less reliable.[33−35] Changes in free-energy terms for translation and rotation are poorly defined in solution, particularly as the size of the molecule increases. Additional corrections to the free energy for concentration differentials among species (to obtain the chemical potential) can be significant, especially if the solubility varies among the different species in solution. Furthermore, because the reactions being studied are in solution, the free energy being accounted for comes from two different sources: thermal corrections and implicit solvent. Neither of these parameters is easily separable nor do they constitute all of the required parts of the free energy under our approximations of the system.

Our reported ΔH values are calculated from the difference in solution-phase enthalpy between the reactants and products. These are calculated by adding to the electronic energies (1) zero-point energy, (2) enthalpic thermal corrections to 298 K and, (3) the free energy due to solvation. It is important to note that even though the solvation energy contribution is to some extent a free-energy correction, it certainly does not account for all of the free energy. Hence, we will retain the symbol ΔH and refer to this quantity as the solution-phase enthalpy in our results and discussion.

For transition states involving condensation reactions (the vertical arrows in Figure 2), we found little change between the gas-phase and implicit solvent-optimized geometries. Therefore, the solvation energy was calculated at the optimized gas-phase transition-state geometry. An additional water molecule was also added when optimizing the condensation reaction transition states because it provided a better network of hydrogen bonding in the transition-state geometries. We also compared the difference in transition-state structure and the corresponding energy barrier in the absence and presence of the extra water molecule. This was another reason that we chose to use water as an implicit solvent in this preliminary study.

TABLE 3: Relative Enthalpies (in kcal/mol) of Reactants, Products, and Intermediates in Solution

	methyl	phenyl
1	0.00	0.00
1·NH$_3$	0.30	0.07
2	5.00	3.17
2a·NH$_3$	−1.13	−0.70
2b·NH$_3$	1.09	1.36
3	12.33	9.97
3a·NH$_3$	3.57	0.57
3b·NH$_3$	4.89	5.39
3c·NH$_3$	7.02	6.48
3r	9.00	6.79
3r·NH$_3$	−0.31	−1.80

For transition states involving the addition of NH_3 to form an adduct (horizontal arrows in Figure 2), the gas-phase and solvent-optimized geometries were quite different. In these cases, we started from the adduct and progressively stretched the B−N bond in 0.1 Å increments. We calculated the solvation energy and the enthalpy corrections (see below) at each of these geometries and identified the transition state as having the largest value of ΔH_{soln} along the reaction coordinate involving the stretching of the B−N bond. Except for the boroxine ring, the explicit hopping barriers were higher than those calculated by adding/removing NH_3.

Results and Discussion

This section is organized as follows. First we will present our thermodynamic calculations of the methyl system and compare it to the phenyl system. Then we will present our kinetic calculations dividing the reactions into three distinct groups.

Thermodynamics of Boroxine·NH$_3$ Formation from Boronic Acid. The enthalpies for all reactions shown in Figure 2 for the methyl system are compiled in Table 1. For comparison, the reaction enthalpies of the phenyl system are compiled in Table 2.

The following trends are observed:

- The dimerization and trimerization reactions are endothermic; the magnitude of ΔH_{soln} is larger for the methyl group.
- Ring closure from **3** to **3r** is exothermic by ∼3 kcal/mol in both cases.
- Addition of NH_3 is marginally endothermic for **1** but exothermic for **2**, **3**, and **3r**; addition to **3** and **3r** are more exothermic than addition to **2**.
- NH_3 prefers the boron attached to an oxygen that is a hydrogen-bond acceptor; the energy gap between **2a·NH$_3$** and **2b·NH$_3$** is ∼2 kcal/mol in both cases; but for the trimer adduct **3a·NH$_3$** is 5−6 kcal/mol more stable than **3b·NH$_3$** and **3c·NH$_3$** for phenyl, whereas this gap is 1−3 kcal/mol for methyl.

To facilitate a comparison of stabilities, we have chosen the Lewis-acid monomer **1** as the reference state. On the basis of the calculated reaction enthalpies in Tables 1 and 2, we can calculate the relative enthalpies of each species. These values are given in Table 3 and displayed graphically in Figure 3, arranged in four "dual" columns differentiated by oligomer size. Adducts and their corresponding Lewis acids are placed in the same column. In each column, the data for phenyl is offset to the right of the data for methyl.

From Figure 3, we see that the open trimer **3** is the least-stable intermediate in solution. Only two species are more stable than **1**, **2a·NH$_3$** and **3r·NH$_3$**. We had previously suggested that **2a·NH$_3$** was the key intermediate prior to forming **3r·NH$_3$**.[23] As expected, **3r·NH$_3$** is the thermodynamic sink for phenyl, but this is not the case for methyl. Besides inherent computational errors due to the choice of method and basis set, there are two other possible explanations. First, the electron-donating methyl group disfavors adduct formation relative to the electron-withdrawing phenyl group.[21] Second, we have not included the entropic contribution that would favor **3r·NH$_3$** over **2a·NH$_3$** because of the release of an additional water molecule upon ring closure forming the boroxine.

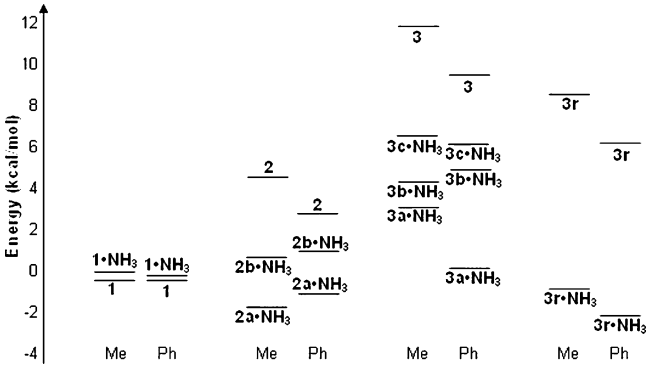

Figure 3. Visual representation of relative enthalpies in solution.

The general trends are similar for both methyl and phenyl, although there are some differences in the relative magnitudes between species in solution. The relative enthalpy between **1** and **1·NH$_3$** is small. In contrast, the Lewis acids **2**, **3**, and **3r** are higher-energy intermediates compared to the adducts containing NH_3. The spread of energies is generally larger comparing species in each column of Figure 3 for methyl compared to phenyl (except for **3** and its adducts, the spread is similar for both methyl and phenyl).

The lowest-enthalpy sequential pathway for both methyl and phenyl, ignoring barriers, is to add NH_3 to **1** forming **1·NH$_3$**. Subsequent addition of **1** to **1·NH$_3$** forms **2a·NH$_3$**. Further addition of **1** forms **3a·NH$_3$**, which then cyclizes to **3r·NH$_3$**. The highest-energy intermediate along this pathway is **3a·NH$_3$** with a relative enthalpy of 3.57 and 0.57 kcal/mol for methyl and phenyl, respectively.

We highlight the similarities and differences in methyl and phenyl because the transition states and energy barriers calculated are for the less computationally expensive methyl, whereas boroxine formation in the phenyl system has been more extensively studied experimentally.

Kinetics of Methylboroxine·NH$_3$ Formation from Methylboronic Acid. We have calculated the transition states and energy barriers for the reactions shown in Figure 2. The transition states are labeled according to Figure 4. The reaction enthalpies from reactant to transition state (forward reaction) and product to transition state (reverse reaction) are compiled in Table 4a and b, respectively. Note that (1) the oligomerization reactions have an additional water molecule added in the transition state and (2) the barriers for NH_3 addition are listed rather than a hopping barrier between nonequivalent sites.

The transition states can be grouped into three categories: (1) hydration/dehydration reactions in the absence of NH_3 involving interconversion between monomer, dimer, trimer, and boroxine (**TS12**, **TS23**, **TS33r**) Lewis acids; (2) addition/elimination of NH_3 to a Lewis acid (**TS1·NH$_3$**, **TS2a·NH$_3$**, **TS2b·NH$_3$**, **TS3a·NH$_3$**, **TS3b·NH$_3$**, **TS3c·NH$_3$**) or NH_3 hopping within an oligomer (**TS3r·NH$_3$**); (3) hydration/dehydration in the presence of NH_3 where at least one of the oligomers is an adduct (**TS12a**, **TS2a3a**, **TS23b**, **TS3a3r**). The relative energies of all of these transition states can be compared to the reactants, products, and intermediates for methyl from Table 3 and Figure 3. These are shown in Table 5 and Figure 5. A

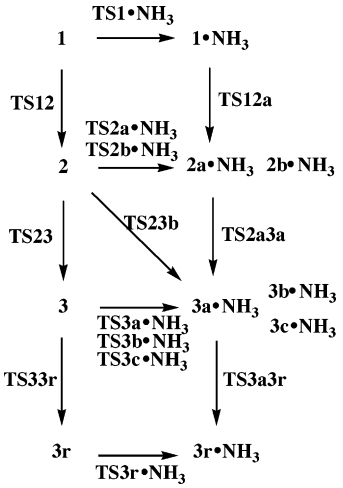

Figure 4. Transition states considered in the conversion of methylboronic acid to the trimethylboroxine·NH_3 adduct.

number of other higher-energy transition states, not part of the potential lowest-energy pathway, were also calculated but not shown in Table 5 and Figure 5.

The transition states of hydration/dehydration reactions in Figure 5 are connected to the reactants and products by curves. Two "pathways" are represented, one for the conversion of **1** → **2** → **3** → **3r** in the absence of NH_3 (red lines), the other (blue lines) involving adducts with NH_3. Transition states involving addition/elimination/hopping of NH_3 are not connected by curves and are grouped in the appropriate columns for monomer, dimer, trimer, and boroxine ring, respectively. We see that hydration/dehydration transition states have higher relative enthalpies than transition states involving addition/elimination/hopping of NH_3. Among the former, those involving adducts have marginally higher relative enthalpies than those without NH_3. Each of these three categories will be discussed in turn.

TABLE 5: Relative Enthalpies (in kcal/mol) of Transition States in Solution (Methyl Only)

reaction	ΔH_{soln} (kcal/mol)
TS12	17.69
TS23	19.92
TS33r	21.08
TS1·NH3	5.82
TS2a·NH3	8.92
TS2b·NH3	10.07
TS3a·NH3	16.33
TS3b·NH3	15.42
TS3c·NH3	16.67
TS3r·NH3	13.73
TS12a	18.70
TS2a3a	21.30
TS23b	20.61
TS3a3r	21.99

The first pathway we will consider is the formation of trimethylboroxine in the absence of NH_3. Stepwise addition of two monomers proceeds via the transition states **TS12** and **TS23** forming the dimer and trimer, respectively. Each condensation step involves extrusion of one water molecule. The final step is cyclization of the trimer to form the boroxine ring proceeding via transition state **TS33r**, also extruding one water molecule. The forward barrier (Table 4a) for each of these successive steps decreases (17.7, 14.9, 8.8 kcal/mol, respectively). However, the relative energy of the transition state with reference to meth-

TABLE 4

(a) Forward-Reaction Energy Barriers of Methylboroxine·NH_3 Formation from Methylboronic Acid

reaction	ΔE_{elec} (kcal/mol)	ΔE_{solv} (kcal/mol)	ΔE_{corr} (kcal/mol)	ΔH_{soln} (kcal/mol)
1 + **1** + H_2O → **TS12**	4.85	13.72	−0.88	17.69
2 + **1** + H_2O → **TS23**	2.80	12.47	−0.35	14.92
3 + H_2O → **TS33r**	3.66	7.04	−1.95	8.75
1 + NH_3 → **TS1·NH3**	−0.25	4.84	1.23	5.82
2 + NH_3 → **TS2a·NH3**	−2.46	5.05	1.33	3.92
2 + NH_3 → **TS2b·NH3**	−1.13	4.87	1.33	5.07
3 + NH_3 → **TS3a·NH3**	−3.35	5.77	1.38	3.80
3 + NH_3 → **TS3b·NH3**	−3.65	5.83	0.91	3.09
3 + NH_3 → **TS3c·NH3**	−1.62	4.69	1.27	4.34
3r + NH_3 → **TS3r·NH3**	−2.55	4.86	2.42	4.73
1 + **1·NH3** + H_2O → **TS12a**	1.17	18.79	−1.56	18.40
1 + **2a·NH3** + H_2O → **TS2a3a**	4.93	18.86	−1.36	22.43
2 + **1·NH3** + H_2O → **TS23b**	−0.70	17.34	−1.03	15.61
3a·NH3 + H_2O → **TS3a3r**	10.51	11.10	−3.19	18.42

(b) Reverse-Reaction Energy Barriers of Methylboroxine·NH_3 Formation from Methylboronic Acid

reaction	ΔE_{elec} (kcal/mol)	ΔE_{solv} (kcal/mol)	ΔE_{corr} (kcal/mol)	ΔH_{soln} (kcal/mol)
2 + 2H_2O → **TS12**	0.60	12.44	−0.35	12.69
3 + 2H_2O → **TS23**	−5.82	13.05	0.37	7.60
3r + 2H_2O → **TS33r**	−1.46	11.63	1.91	12.08
1·NH3 → **TS1·NH3**	−1.26	7.10	−0.33	5.51
2a·NH3 → **TS2a·NH3**	1.81	8.53	−0.28	10.06
2b·NH3 → **TS2b·NH3**	0.87	8.74	−0.62	8.99
3a·NH3 → **TS3a·NH3**	1.52	10.46	−0.75	11.23
3b·NH3 → **TS3b·NH3**	1.22	10.52	−1.22	10.52
3c·NH3 → **TS3c·NH3**	0.45	9.25	−0.05	9.65
3r·NH3 → **TS3r·NH3**	4.49	11.28	−1.73	14.04
2a·NH3 + 2H_2O → **TS12a**	2.19	18.73	−1.08	19.84
3a·NH3 + 2H_2O → **TS2a3a**	−1.02	20.21	−1.46	17.73
3a·NH3 + 2H_2O → **TS23b**	−1.38	19.91	−1.18	17.35
3r·NH3 + 2H_2O → **TS3a3r**	5.49	17.86	−1.05	22.30

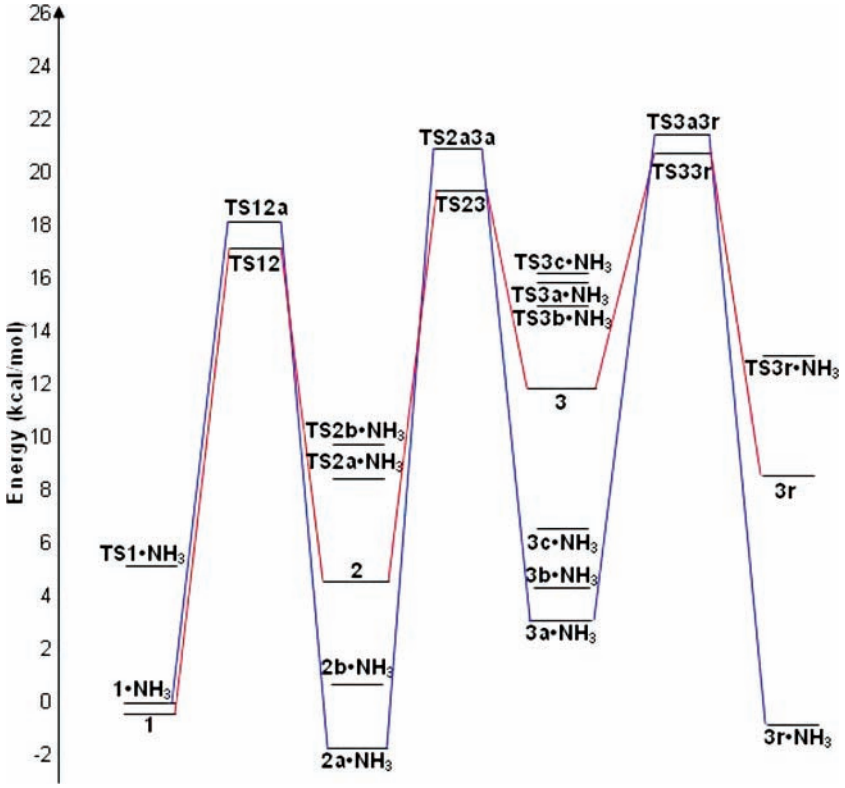

Figure 5. Visual representation of relative energies (in kcal/mol) of intermediates and transition states in solution (methyl only).

TABLE 6: Transition-State Bond Distances (Å) for Figure 7

	TS12	TS23	TS33r		dimer TS	trimer TS
a1	1.113	1.092	1.128	d1	1.200	1.210
a2	1.127	1.119	1.101	d2	1.243	1.268
b1	1.350	1.384	1.324	e1	1.583	1.646
b2	1.324	1.336	1.374	e2	1.568	1.581
c1	1.562	1.538	1.584			
c2	1.559	1.593	1.528			

ylboronic acid (Table 5 and Figure 5) increases marginally for each successive step (17.7, 19.9, 21.1 kcal/mol, respectively). This is because intermediates **2** and **3** are 5.0 and 12.3 kcal/mol relatively higher in energy than **1**.

These three transition states are shown in Figure 6. Note that all three transition states have an additional water molecule added to form a six-center-ring transition state. As the new B−O bond is forming, one of the hydrogens hops to the water molecule forming a H_3O moiety. The transition state is rather symmetrical in terms of the B−O and O−H distances in the six-center ring. Without the additional water molecule, the reaction goes through a four-center transition state and the barriers are substantially higher, 29.7 instead of 17.7 kcal/mol for dimerization of **1** + **1** → **TS12** and 25.8 instead of 14.9 kcal/mol for **1** + **2** → **TS23**.

A schematic of the six- and four-center transition states is shown in Figure 7. Relevant transition-state bond distances are shown in Table 6. For reference, the O−H bond distance in water is 0.964 Å, the O−H bond in **1**, **2**, and **3** ranges from 0.962 to 0.969 Å, and the B−O bond in **1**, **2**, **3**, and **3r** ranges from 1.359 to 1.401 Å. In the six-center transition state, the O−H bonds that are part of the H_3O moiety (a1 and a2) are only ∼0.15 Å longer than the equilibrium O−H bonds. The other two O−H bonds that are breaking and forming (b1 and b2) are in the 1.3−1.4 Å range. The B−O bonds (c1 and c2) are ∼0.2 Å longer than the equilibrium B−O bonds.

If methyl were substituted with phenyl for the dimerization reaction, then the calculated energy barrier is 17.6 kcal/mol instead of 17.7 kcal/mol, suggesting that there may be little difference in barriers between methyl and phenyl for condensation/hydrolysis reactions (in the absence of a Lewis base).

Next, we consider reactions involving the addition/elimination of NH_3. For addition of NH_3 to **1**, the barrier is only 5.8 kcal/mol. The B−N distance is 2.4 Å, much longer than the equilibrium B−N bond length in the adduct that ranges from 1.705 to 1.797 Å (from **3r·NH$_3$** to **1·NH$_3$**, respectively). This is because the major contributor to the barrier, the desolvation penalty in bringing the two separated molecules together to form an adduct, is not compensated by any stabilizing intermolecular interactions (e.g., hydrogen bonds in the case of bringing oligomers and/or water together).

For the dimers and trimers, the forward barriers are all small (3.1 to 5.8 kcal/mol). The reverse barriers, for removing NH_3 from the adduct, are directly related to the binding energy of NH_3, as expected. As in **TS1·NH$_3$**, the B−N distances in the transition state are all long; 2.6 Å for both **TS2a·NH$_3$** and **TS2b·NH$_3$**, 3.0 Å for **TS3a·NH$_3$**, 2.5 Å for **TS3b·NH$_3$**, and 2.8 Å for **TS3c·NH$_3$**. As discussed in the Computational Methods section, transition states were located starting from the adduct and progressively stretching the B−N bond. In the dimer and trimer, NH_3 hopping was not observed. When forcing the reaction coordinate to trace a path from one boron to the other, we were able to locate hopping transition states but they all had higher barriers than those for removing NH_3. Hence, we have not included them here. (The reason is that the transition states involve significant compression distorting the B−O−B angle.) There is one exception: **TS3r·NH$_3$**. Starting from **3r·NH$_3$** and stretching the B−N bond, the transition state had all three B−N distances roughly equidistant (3.34 to 3.37 Å). This hopping barrier is 14.0 kcal/mol. The rigidity of the ring prevents distortion of the B−O−B angles in this case.

As mentioned earlier, there is little experimental data on energy barriers in this system. The hopping barrier measured by ^{1}H NMR for for piperidine on trimethylboroxine (in CD_2-

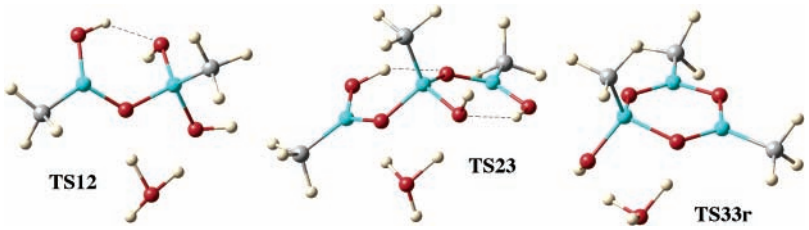

Figure 6. Lewis-acid transition states for condensation/hydrolysis reactions.

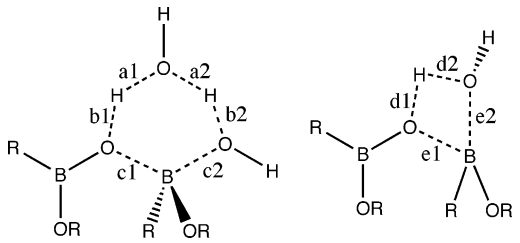

Figure 7. Schematic of six- and four-center transition states.

Cl_2) was 10.3 kcal/mol.[24] We calculated the same system in the same solvent and found the barrier to be 10.0 kcal/mol. However, our calculated barrier for pyridine on triphenylboroxine is 10.8 kcal/mol, slightly higher than the ^{1}H NMR measured barrier of 9.3 kcal/mol.[15] Note that we have not included entropic effects in our calculations.

To see the effect of using a different base, we calculated the transition state for adding pyridine rather than NH_3 to **1**. The B−N distance in the transition state is 2.4 Å, similar to NH_3. The barrier is 2.4 kcal/mol, which is lower than the 5.8 kcal/mol found for NH_3. This difference is approximately the same order of magnitude (∼2 kcal/mol) as the binding-energy difference between NH_3 and pyridine (pyridine binds weaker).[21]

If methyl is replaced with phenyl with NH_3 as the ligand, then the transition state has a B−N distance of 2.5 Å, and the barrier is 5.8 kcal/mol (similar to methyl). This is not surprising because the enthalpy change for the addition of NH_3 to **1** is similar (0.3 and 0.1 kcal/mol) in both methyl and phenyl.

The final pathway we will consider is the formation of **3r·NH$_3$** from reactants in the presence of NH_3. The first step involves the addition of **1** and **1·NH$_3$** to form **2a·NH$_3$**, going through transition state **TS12a**. Transition states leading to the formation of **2b·NH$_3$** had higher barriers and are not included here. **TS12a** has the similar six-center transition-state motif we saw in **TS12** with the H_3O moiety. One important difference, however, is that NH_3 forms an intramolecular hydrogen bond. Attempts to rotate the NH_3 group away and form the expected intramolecular hydrogen bond with hydroxyl either resulted in a higher-energy transition state or the B−O bond would rotate and restore the hydrogen bond with NH_3. This is also observed in the transition states for the next two steps: trimerization (**1** and **2a·NH$_3$** to form **3a·NH$_3$** going through **TS2a3a**) and cyclization (**3a·NH$_3$** to **3r·NH$_3$** going through **TS3a3r**). All attempts to optimize transition states to or from higher-energy intermediates (such as **2b·NH$_3$**, **3b·NH$_3$**, **3c·NH$_3$**) resulted in higher-energy transition states with one exception: the addition of **2** and **1·NH$_3$** to form **3b·NH$_3$** going through **TS23b**. These transition states are shown in Figure 8.

The forward and reverse reaction barriers are all larger in magnitude compared to those found in the absence of NH_3 for the **1** → **2** → **3** → **3r** pathway as shown in Table 4a and b. However, because the adducts are lower in energy than the corresponding molecules without NH_3, we see that the transition-state adducts are just marginally higher in energy than those without NH_3 (Figure 5 and Table 5). **TS23b**, not shown in Figure 5, lies in between **TS23** and **TS2a3a**.

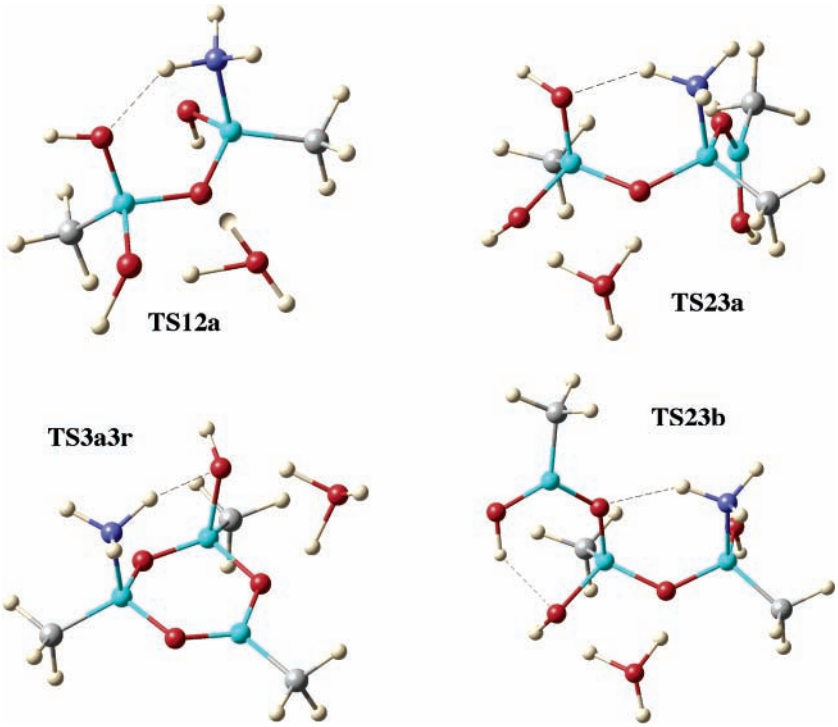

Figure 8. Adduct transition states for condensation/hydrolysis reactions.

From Figure 5, it is clear that the relative transition-state energies for addition or removal of NH_3 are significantly lower than those for the hydration/dehydration reactions. Hence, we expect fast exchange for adding and removing the base and by extension hopping of the base between boron sites in dimers, trimers, and the boroxine ring. The relative transition-state energies for hydration/dehydration reactions for the adduct are all marginally higher than those for the Lewis acids in the absence of NH_3. The barriers involving the adduct are higher because the adduct intermediates are more stable than the Lewis-acid intermediates. The lowest-energy pathway to transform **1** to **3r·NH$_3$** is therefore dimerization, trimerization, and ring closure of the Lewis acids going through high-energy intermediates **2** and **3**. At the same time, fast addition or removal of NH_3 throughout the entire process is expected. In fact, the role of the base may be to help stabilize the dimer and trimer against simply hydrolyzing back to the monomer.

Given the interest in utilizing arylboroxines in material-science applications,[17−19] while we have not explicitly calculated all the transition states, we predict what to expect in the formation of triphenylboroxine from boronic acid in the presence of pyridine. From Figure 3, we have seen that the Lewis-acid intermediates are relatively lower in energy for phenyl compared to methyl. As the Lewis acidity increases, because of the electron withdrawing phenyl group, the corresponding adduct also becomes more stable (e.g., **3a·NH$_3$** and **3r·NH$_3$**). We have seen that pyridine binds weaker than NH_3 [20] and that the barrier for addition/removal/hopping of pyridine is lower than that for NH_3. We also found that the dimerization of monomers to form **2** has approximately the same forward reaction barrier for methyl and phenyl. However, because the relative stability of **2** to **1** in phenyl and methyl are different (formation of **2** being less-endothermic for phenyl), the reverse reaction barrier would be higher for phenyl. And because the Lewis-acid intermediates (**2**, **3**, **3r**) for phenyl in Figure 3 are correspondingly more stable than their methyl counterparts by 2−3 kcal/mol, we also expect their relative transition-state energies to be lower. In fact, extrapolation from our limited data set would suggest that for phenyl the relative transition-state energies for both **TS23** and **TS33r** would be ∼18 kcal/mol, close to **TS12** (17.6 kcal/mol) and that the mechanism should be similar.

Conclusions

From our DFT calculations for the conversion of methylboronic acid into the trimethylboroxine·NH_3 adduct, the most-stable intermediate is the dimer adduct (**2a·NH$_3$**). With the exception of the monomer, all adducts were thermodynamically favored over the corresponding Lewis acids. Where there was a choice of different sites for NH_3, the most-stable adduct had NH_3 binding to the most acidic boron. Fast addition/removal/hopping of NH_3 is expected because the calculated relative energy barriers are significantly lower than those for condensation/hydrolysis. The lowest-energy pathway still goes through condensation/hydrolysis of the Lewis acids, although the pathway involving adduct condensation/hydrolysis is very close in energy (certainly within the computational error of the method and basis set).

Our calculations suggest that the conversion of phenylboronic acid into the triphenylboroxine·pyridine adduct is both thermodynamically and kinetically more favorable than that for methyl. Faster exchange is expected in the weaker-binding pyridine compared to NH_3. The condensation/hydrolysis reactions are still expected to be the rate-determining step.

Acknowledgment. This research was supported by the Camille and Henry Dreyfus Foundation Start-up Award and an award from Research Corporation. We thank Dr. Peter Iovine for helpful discussions.

Supporting Information Available: Calculated values of E_{elec}, E_{solv}, and E_{corr}. This material is available free of charge via the Internet at http://pubs.acs.org.

References and Notes

(1) *Boronic Acids: Preparation and Applications in Organic Synthesis and Medicine*; Hall, D. G., Ed.; Wiley-VCH: Weinheim, Germany, 2005.

(2) Morgan, A. B.; Jurs, J. L.; Tour, J. M. *Polym. Prepr. (Am. Chem. Soc., Div. Polym. Chem.)* **1999**, *40*, 553.

(3) Mehta, M. A.; Fujinami, T. *Chem. Lett.* **1997**, 915.

(4) Yang, Y.; Inoue, T.; Fujinami, T.; Mehta, M. A. *J. Appl. Polym. Sci.* **2002**, *84*, 17−21.

(5) Forsyth, M.; Sun, J.; Zhou, F.; MacFarlane, D. R. *Electrochim. Acta* **2003**, *48*, 2129.

(6) Miyaura, N.; Suzuki, A. *Chem. Rev.* **1995**, *95*, 2457.

(7) Alcaraz, G.; Euzenat, L.; Mongin, O.; Katan, C.; Ledoux, I.; Zyss, J.; Blanchard-Desce, M.; Vaultier, M. *Chem. Commun.* **2003**, *22*, 2766.

(8) Fielder, W. L.; Chamberlain, M. M.; Brown, C. A. *J. Org. Chem.* **1961**, *26*, 2154.

(9) Branch, G. E. K.; Yabroff, D. L. *J. Am. Chem. Soc.* **1932**, *54*, 2569.

(10) Mariategui, J. F.; Niedenzu, K. *J. Organomet. Chem.* **1989**, *369*, 137.

(11) Beckett, M. A.; Strickland, G. C.; Varma, K. S.; Hibbs, D. E.; Hursthouse, M. B.; Malik, K. M. A. *J. Organomet. Chem.* **1997**, *535*, 33.

(12) Ritchey, J. M. Synthesis and Properties of Addition Complexes of Boroxines and Other Selected Boron-Containing Systems. Ph.D. Thesis, University of Colorado, 1968.

(13) Snyder, H. R.; Konecky, M. S.; Lennarz, W. J. *J. Am. Chem. Soc.* **1958**, *80*, 3611.

(14) Das, M. K.; Mariategui, J. F.; Niedenzu, K. *Inorg. Chem.* **1987**, *26*, 3114.

(15) Wu, Q. G.; Wu, G.; Brancaleon, L.; Wang, S. *Organometallics* **1999**, *18*, 2553.

(16) Vargas, G.; Hernandez, I.; Hopfl, H.; Ochoa, M.-E.; Castillo, D.; Farfan, N.; Santillan, R.; Gomez, E. *Inorg. Chem.* **2004**, *43*, 8490.

(17) Cote, A. P.; Benin, A. I.; Ockwig, N.; O'Keefe, M.; Matzger, A. J.; Yaghi, O. M. *Science* **2005**, *310*, 1166.

(18) Qin, Y.; Cui, C.; Jäkle, F. *Macromolecules* **2007**, *40*, 1413.

(19) Iovine, P. M.; Fletcher, M. N.; Lin, S. *Macromolecules* **2006**, *39*, 6324.

(20) Tokunaga, Y.; Ueno, H.; Shimomura, Y.; Seo, T. *Heterocycles* **2002**, *57*, 787.

(21) Kua, J.; Iovine, P. M. *J. Phys. Chem. A* **2005**, *109*, 8938.

(22) Beckmann, J.; Dakternieks, D.; Duthie, A.; Lim, A. E. K.; Tiekink, E. R. T. *J. Organomet. Chem.* **2001**, *633*, 149.

(23) Kua, J.; Fletcher, M. N.; Iovine, P. M. *J. Phys. Chem. A* **2006**, *110*, 8158.

(24) Beckett, M. A.; Brassington, D. S.; Owen, P.; Hursthouse, M. B.; Light, M. E.; Malik, K. M. A.; Varma, K. S. *J. Organomet. Chem.* **1999**, *585*, 7.

(25) Beckett, M. A.; Hibbs, D. E.; Hursthouse, M. B.; Owen, P.; Malik, K. M. A.; Varma, K. S. *Main Group Chem.* **1998**, *2*, 251.

(26) *Jaguar*, v6.0; Schrodinger, LLC: Portland, OR, 2005.

(27) Becke, A. D. *J. Chem. Phys.* **1993**, *98*, 5648.

(28) Becke, A. D. *Phys. Rev. A* **1988**, *38*, 3098.

(29) Vosko, S. H.; Wilk, L.; Nusair, M. *Can. J. Phys.* **1980**, *58*, 1200.

(30) Lee, C.; Yang, W.; Parr, R. G. *Phys. Rev. B* **1988**, *37*, 785.

(31) Tannor, D. J.; Marten, B.; Murphy. R.; Friesner, R. A.; Sitkoff, D.; Nicholls, A.; Ringnalda, M.; Goddard, W. A., III.; Honig, B. *J. Am. Chem. Soc.* **1994**, *116*, 11875.

(32) Marten, B.; Kim, K.; Cortis, C.; Friesner, R. A.; Murphy, R. B.; Ringnalda, M. N.; Sitkoff, D.; Honig, B. *J. Phys. Chem.* **1996**, *100*, 11775.

(33) Wiberg, K. B.; Bailey, W. F. *J. Am. Chem. Soc.* **2001**, *123*, 8231.

(34) Nielsen, R. J.; Keith, J. M.; Stoltz, B. M.; Goddard, W. A., III. *J. Am. Chem. Soc.* **2004**, *126*, 7967.

(35) Florian, J.; Warshel, A. *J. Phys. Chem. B* **1998**, *102*, 719.